tions of the sialidases inside the cells nor the sialidase activity following exogenous addition of substrates.

DISCUSSION

In the present study, we explored the inhibitory effects of oseltamivir and zanamivir on four human sialidases using their recombinant proteins. The effects were examined by two methods, namely, measurement of the inhibitory activity in sialidase activity assays and estimation of the reduced desialylation of endogenous glycoprotein and glycolipid substrates inside the cells. Recent observations have suggested a possible inhibitory potential of oseltamivir against endogenous sialidases. In mice, the drug decreased the GM1 of activated $CD8^+$ T cells infected with a respiratory syncytial virus (18) and also blocked GM1-mediated opioid hyperalgesia induced by low doses of morphine (5). In rats, it exhibited neuroexcitatory effects, especially under conditions of simultaneous administration of ethanol (10). With these animal models, however, no direct inhibitory effects of the drugs on endogenous sialidases could be shown. We do not yet know the molecular mechanisms underlying these phenomena at present, but our data suggest that they may not be the direct consequences of sialidase inhibition. Decreased GM1 may not always be due to sialidase inhibition and may also involve other processes, such as disturbance of the ganglioside synthetic pathway. In a report on the effects of the drugs on the sialidases of PC12 cells, Tamiflu was found to inhibit the sialidase activity induced by nerve growth factor-dependent Trk receptor activation (29). Although we tried to examine the inhibitory effects under the same experimental conditions and confirmed induction of sialidase activity toward 4MU-NeuAc in a nerve growth factor-dependent manner, we were not able to detect any inhibition of the activity in the cells at a Tamiflu dose of 1 mM. This ineffectiveness of Tamiflu is probably due to the absence or low expression of carboxyesterase 1 (23) and P-glycoprotein (19) in the cells, which are involved in activation and transport of the prodrug oseltamivir, respectively. Studies using recombinant NEU2 sialidase (11) have shown that a variant with a nonsynonymous single nucleotide polymorphism frequently observed in some Asian populations is associated with lower sialidase activity and higher sensitivity to oseltamivir than the wild-type enzyme. This is of particular interest in the context of the frequent occurrence of abnormal behavior and deaths associated with Tamiflu use in Japan. However, in addition to the extremely low expression of NEU2 in human tissues, including the brain, as shown in Fig. 1, our present data demonstrate that very high concentrations of oseltamivir carboxylate are needed to inhibit the sialidase activity, which is 14- to 20-fold higher than the concentration reported by Li et al. (11). The other sialidases were not susceptible to the drug, even in the millimolar range, despite the drug inhibiting viral sialidases in the nanomolar range. In contrast, zanamivir inhibited NEU3 at micromolar levels. In consistency with this, Nan et al. (20) reported that less than 1 mM zanamivir inhibited the endogenous sialidase activity of human T lymphocytes, although no information is available with regard to the type of sialidase involved in this phenomenon.

Taken together, the data indicate that oseltamivir carboxylate does not significantly inhibit constitutively expressed NEU1, NEU3, or NEU4 human sialidases while zanamivir exhibits inhibitory effects in the micromolar range against NEU3 as the most sensitive form. We cannot arrive at any firm conclusions at present regarding the potential association between Tamiflu and the abnormal behavior and deaths reported among Japanese teenagers with influenza virus infection treated with the drug, but our results do indicate that the drug might not exert any direct effects on the ganglioside-specific plasma membrane-associated sialidase NEU3, expressed abundantly in the brain. The present results were obtained with only recombinant enzymes, and we also need to stress that the observed effects might not directly reflect the effects that might be observed under physiological conditions inside the cells. Since the plasma concentration of oseltamivir carboxylate is reported to be 1.2 μM following oral administration of the 75-mg capsule twice daily to patients (http://www.rocheusa.com/products/tamiflu/), endogenous sialidase is unlikely to be a direct target molecule. In the case of zanamivir, the plasma concentration is observed to be 0.05 to 0.43 μM within 1 to 2 h following administration of a 10-mg dose (http://us.gsk.com/products/assets/us_relenza.pdf). Our results also suggest negligible effects, although it should be borne in mind that the concentration in the respiratory tract after inhalation may be much higher than that achieved in the blood. In conclusion, it may be desirable to examine newly discovered drugs targeting viral sialidases for their effects on endogenous human sialidases, in order to minimize potential side effects in patients.

REFERENCES

1. Anonymous. 2007. New concerns about oseltamivir. Lancet 369:1056.
2. Anonymous. 2007. Japan's health ministry calls for tests on Tamiflu. Nature 447:626–627.
3. Chavas, L. M., C. Tringali, P. Fusi, B. Venerando, G. Tettamanti, R. Kato, E. Monti, and S. Wakatsuki. 2005. Crystal structure of the human cytosolic sialidase Neu2. Evidence for the dynamic nature of substrate recognition. J. Biol. Chem. 280:469–475.
4. Corfield, T. 1992. Bacterial sialidases—roles in pathogenicity and nutrition. Glycobiology 2:509–521.
5. Crain, S. M., and K. F. Shen. 2004. Neuraminidase inhibitor, oseltamivir blocks GM1 ganglioside-regulated excitatory opioid receptor-mediated hyperalgesia, enhances opioid analgesia and attenuates tolerance in mice. Brain Res. 995:260–266.
6. Fuyuno, I. 2007. Tamiflu side effects come under scrutiny. Nature 446:358–359.
7. Galjart, N. J., N. Gillemans, A. Harris, G. T. van der Horst, F. W. Verheijen, and A. d'Azzo. 1988. Expression of cDNA encoding the human "protective protein" associated with lysosomal beta-galactosidase and neuraminidase: homology to yeast proteases. Cell 54:755–764.
8. Gubareva, L. V., L. Kaiser, and F. G. Hayden. 2000. Influenza virus neuraminidase inhibitors. Lancet 355:827–835.
9. Hama, R. 2007. Fifty sudden deaths may be related to central suppression. BMJ 335:59.
10. Izumi, Y., K. Tokuda, K. A. O'Dell, C. F. Zorumski, and T. Narahashi. 2007. Neuroexcitatory actions of Tamiflu and its carboxylate metabolite. Neurosci. Lett. 426:54–58.
11. Li, C. Y., Q. Yu, Z. Q. Ye, Y. Sun, Q. He, X. M. Li, W. Zhang, J. Luo, X. Gu, X. Zheng, and L. Wei. 2007. A nonsynonymous SNP in human cytosolic sialidase in a small Asian population results in reduced enzyme activity: potential link with severe adverse reactions to oseltamivir. Cell Res. 17:357–362.
12. Maxwell, S. R. 2007. Tamiflu and neuropsychiatric disturbance in adolescents. BMJ 334:1232–1233.
13. Milner, C. M., S. V. Smith, M. V. Carrillo, G. L. Taylor, M. Hollinshead, and R. D. Campbel. 1997. Identification of a sialidase encoded in the human major histocompatibility complex. J. Biol. Chem. 272:4549–4558.
14. Miyagi, T., K. Konno, Y. Emori, H. Kawasaki, K. Suzuku, A. Yasui, and S. Tsuiki. 1993. Molecular cloning and expression of cDNA encoding rat skeletal muscle cytosolic sialidase. J. Biol. Chem. 268:26435–26440.
15. Miyagi, T., and K. Yamaguchi. 2007. Biochemistry of glycans: sialic acids, p. 297–322. *In* J. P. Kamerling, G. Boons, Y. C. Lee, A. Suzuki, N. Taniguchi, and A. G. J. Voragen (ed.), Comprehensive glycoscience. Elsevier BV, Amsterdam, The Netherlands.

16. Miyagi, T., T. Wada, K. Yamaguchi, and K. Hata. 2004. Sialidase and malignancy: a minireview. Glycoconj. J. 20:189–198.
17. Monti, E., A. Preti, E. Rossi, A. Ballabio, and G. Borsani. 1999. Cloning and characterization of Neu2, a human gene homologous to rodent soluble sialidases. Genomics 57:137–143.
18. Moore, M. L., M. H. Chi, W. Zhou, K. Goleniewska, J. F. O'Neal, J. N. Higginbotham, and R. S. Peebles, Jr. 2007. Oseltamivir decreases T cell GM1 expression and inhibits clearance of respiratory syncytial virus: potential role of endogenous sialidase in antiviral immunity. J. Immunol. 178:2651–2654.
19. Morimoto, K., M. Nakakariya, Y. Shirasaka, C. Kakinuma, T. Fujita, I. Tamai, and T. Ogihara. 2008. Oseltamivir (Tamiflu) efflux transport at the blood-brain barrier via P-glycoprotein. Drug Metab. Dispos. 36:6–9.
20. Nan, X., I. Carubelli, and N. M. Stamatos. 2007. Sialidase expression in activated human T lymphocytes influences production of IFN-gamma. J. Leukoc. Biol. 81:284–296.
21. Potier, M., L. Mameli, M. Belisle, L. Dallaire, and S. B. Melancon. 1979. Fluorometric assay of neuraminidase with a sodium (4-methylumbelliferyl-alpha-D-N-acetylneuraminate) substrate. Anal. Biochem. 94:287–296.
22. Roggentin, P., B. Rothe, J. B. Kaper, J. Galen, L. Lawrisuk, E. R. Vimr, and R. Schauer. 1989. Conserved sequences in bacterial and viral sialidases. Glycoconj. J. 6:349–353.
23. Shi D., J. Yang, D. Yang, E. L. LeCluyse, C. Black, L. You, F. Akhlaghi, and B. Yan. 2006. Anti-influenza prodrug oseltamivir is activated by carboxylesterase human carboxylesterase 1, and the activation is inhibited by antiplatelet agent clopidogrel. J. Pharmacol. Exp. Ther. 319:1477–1484.
24. Suzuki, Y., Y. Nagano, H. Kato, M. Matsumoto, K. Nerome, K. Nakajima, and E. Nobusawa. 1986. Human influenza A virus hemagglutinin distinguishes sialyloligosaccharides in membrane-associated gangliosides as its receptor which mediates the adsorption and fusion processes of virus infection. Specificity for oligosaccharides and sialic acids and the sequence to which sialic acid is attached. J. Biol. Chem. 261:17057–17061.
25. von Itzstein, M. 2007. The war against influenza: discovery and development of sialidase inhibitors. Nat. Rev. Drug Discov. 6:967–974.
26. von Itzstein, M., W. Y. Wu, G. B. Kok, M. S. Pegg, J. C. Dyason, B. Jin, T. van Phan, M. L. Smythe, H. F. White, and S. W. Oliver. 1993. Rational design of potent sialidase-based inhibitors of influenza virus replication. Nature 363:418–423.
27. Wada, T., K. Hata, K. Yamaguchi, K. Shiozaki, K. Koseki, S. Moriya, and T. Miyagi. 2007. A crucial role of plasma membrane-associated sialidase (NEU3) in the survival of human cancer cells. Oncogene 26:2483–2490.
28. Wada, T., Y. Yoshikawa, S. Tokuyama, M. Kuwabara, H. Akita, and T. Miyagi. 1999. Cloning, expression and chromosomal mapping of a human ganglioside sialidase. Biochem. Biophys. Res. Commun. 261:21–27.
29. Woronowicz, A., S. R. Amith, K. De Vusser, W. Laroy, R. Contreras, S. Basta, and M. R. Szewczuk. 2007. Dependence of neurotrophic factor activation of Trk tyrosine kinase receptors on cellular sialidase. Glycobiology. 17:10–24.
30. Yamaguchi, T., K. Hata, K. Koseki, K. Shiozaki, H. Akita, T. Wada, S. Moriya, and T. Miyagi. 2005. Evidence for mitochondrial localization of a novel human sialidase (NEU4). Biochem. J. 390:85–93.

Available online at www.sciencedirect.com
ScienceDirect
Nuclear Medicine and Biology 36 (2009) 47–55
NUCLEAR MEDICINE — AND — BIOLOGY
www.elsevier.com/locate/nucmedbio

Biodistribution and metabolism of the anti-influenza drug [^{11}C]oseltamivir and its active metabolite [^{11}C]Ro 64-0802 in mice

Akiko Hatori, Takuya Arai, Kazuhiko Yanamoto, Tomoteru Yamasaki, Kazunori Kawamura, Joji Yui, Fujiko Konno, Ryuji Nakao, Kazutoshi Suzuki, Ming-Rong Zhang*

Department of Molecular Probes, Molecular Imaging Center, National Institute of Radiological Sciences (NIRS), Inage-ku, Chiba 263-8555, Japan

Received 22 July 2008; received in revised form 10 October 2008; accepted 15 October 2008

Abstract

Introduction: Oseltamivir phosphate (Tamiflu) is an orally active anti-influenza drug, which is hydrolyzed by esterase to its carboxylate metabolite Ro 64-0802 with potent activity to inhibit the influenza virus. The abnormal behavior and death associated with the use of oseltamivir have developed into a major problem in Japan where Tamiflu is often prescribed for seasonal influenza. It is critical to determine the amount of oseltamivir and Ro 64-0802 in the human brain and to elucidate the relationship between their amounts and neuropsychiatric side effects. The aim of this study was to evaluate [^{11}C]oseltamivir and [^{11}C]Ro 64-0802 in mice as promising positron emission tomography (PET) ligands for measuring their amounts in living brains.

Methods: Whole-body biodistribution of [^{11}C]oseltamivir and [^{11}C]Ro 64-0802 was determined in mice using the dissection method and micro-PET. In vitro and in vivo metabolite assay was performed in the plasma and brain of mice.

Results: Between 1 and 60 min after injection of [^{11}C]oseltamivir and [^{11}C]Ro 64-0802, 0.20–0.06% and 0.39–0.03% ID/g were detected in the mouse brains, respectively (dissection method). Radioactivity concentrations in the living brains between 0 and 90 min after injection were measured at standardized uptake values of 0.25–0.05 for [^{11}C]oseltamivir and 0.38–0.02 for [^{11}C]Ro 64-0802 (micro-PET). In vivo metabolite assay demonstrated the presence of [^{11}C]oseltamivir and [^{11}C]Ro 64-0802 in the brains after [^{11}C]oseltamivir injection.

Conclusion: This study determined the distribution and metabolism of [^{11}C]oseltamivir and [^{11}C]Ro 64-0802 in mice. PET could be used to measure their amounts in the living brain and to elucidate the relationship between the amounts in the brain and the side effects of Tamiflu in the central nervous system.

Keywords: Anti-influenza drug; [^{11}C]Oseltamivir; [^{11}C]Ro 64-0802; Micro-PET; Brain uptake

1. Introduction

Oseltamivir phosphate (Tamiflu, Fig. 1) is an orally active anti-influenza drug for the treatment of influenza types A and B [1–3]. It is a prodrug that is hydrolyzed by esterase to its carboxylate metabolite Ro 64-0802 (Fig. 1), a potent inhibitor of the influenza virus [4–6]. This drug is regularly prescribed as a treatment for seasonal influenza in Japan, and Japanese consumption accounts for up to 75% of all Tamiflu use worldwide. However, the safety of oseltamivir has been questioned because suicidal or abnormal behavior, especially in young patients, has been reported after Tamiflu ingestion [7].

At present, the Japan label of the drug specifies that the drug should not be administrated to young patients as there is a possible risk of neurological adverse effects [8], but the mechanisms of this abnormal behavior are uncertain. Oseltamivir may affect the central nervous system (CNS) because neuraminidase, a key enzyme relative to the proliferation of influenza virus inhibited by Ro 64-0802, plays a role in CNS development and impulse conduction [9–11]. In vitro study on brain slices demonstrated that Ro 64-0802 had clear effects on neuronal excitability and oseltamivir enhanced hippocampal network synchronization [12,13]. A high dose of oseltamivir damaged the brain of experimental animals and was likely caused by uptake of

* Corresponding author. Tel.: +81 43 206 4041; fax: +81 43 206 3261.
E-mail address: zhang@nirs.go.jp (M.-R. Zhang).

0969-8051/$ – see front matter © 2009 Elsevier Inc. All rights reserved.
doi:10.1016/j.nucmedbio.2008.10.008

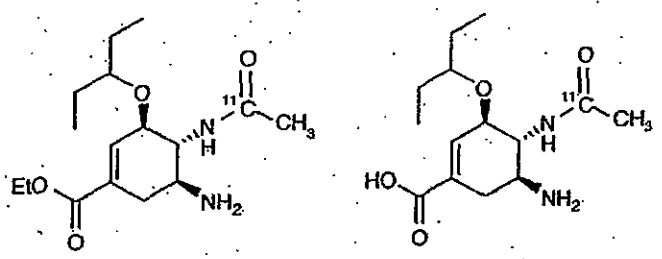

Fig. 1. Chemical structures of [^{11}C]oseltamivir and [^{11}C]Ro 64-0802.

oseltamivir and/or Ro 64-0802 into the CNS. Thus, although it is believed that the two compounds do not easily pass the blood–brain barrier (BBB), they may enter the brain if the BBB is immature or damaged [14]. However, the presence and amounts of oseltamivir and Ro 64-0802 in the human brain, and the relationship between their presence and the side effects of Tamiflu, have not been elucidated clearly [15–18].

Positron emission tomography (PET) is a useful imaging modality employing radioactive ligands labeled with positron-emitting radioactive isotopes, such as carbon-11 (^{11}C; half life: 20.3 min), fluorine-18, nitrogen-13 and oxygen-15 [19]. PET can be used to provide pharmacokinetic and pharmacodynamic information about a drug to determine drug efficacy and potential biochemical mechanisms of drug action, including the adverse and toxic effects. Since influenza is a serious seasonal illness, especially in the winter, and Tamiflu is the first-choice drug [20,21], it is critical to determine the presence and amount of oseltamivir and Ro 64-0802 in the human brain and to explore the relationship between their uptake and side effects on the brain. The effectiveness of PET on the living body prompted us to label oseltamivir and Ro 64-0802 with a positron emitter isotope and to measure their amounts in brains using radiolabeled ligands.

We have recently synthesized [^{11}C]oseltamivir and [^{11}C] Ro 64-0802 and determined their presence in mouse brains using the dissection method [22]. Here, to aim their clinical usefulness, we performed a detailed preclinical evaluation of [^{11}C]oseltamivir and [^{11}C]Ro 64-0802, respectively. Using a dissection method and a small-animal PET (micro-PET), we determined the biodistribution of [^{11}C]oseltamivir and [^{11}C] Ro 64-0802 in various organs of the mouse, including the brain. To elucidate the putative influence of radioactive metabolites on PET imaging and data analysis, we then examined the metabolism of [^{11}C]oseltamivir and [^{11}C]Ro 64-0802 in the brain and the plasma of mice.

2. Materials and methods

2.1. General

Oseltamivir phosphate was purchased from Sequoia Research Products (Pangbourne, UK). Ro 64-0802 was synthesized by hydrolyzing oseltamivir with 1% NaOH solution in our laboratory. All chemicals and solvents were of analytic or high-performance liquid chromatography (HPLC) grade from Aldrich (Milwaukee, WI) and Wako Pure Industries (Osaka, Japan). Carbon-11 was produced by ^{14}N(p, α)^{11}C nuclear reaction using CYPRIS HM18 cyclotron (Sumitomo Heavy Industry, Tokyo, Japan). A dose calibrator (IGC-3R Curiemeter; Aloka, Tokyo, Japan) was used for all radioactivity measurements if not otherwise stated. Reverse-phase HPLC was performed using a JASCO (JASCO, Tokyo, Japan) system: effluent radioactivity was determined using a NaI (Tl) scintillation detector system.

2.2. Production of [^{11}C]oseltamivir and [^{11}C]Ro 64-0802

Radiosynthesis of [^{11}C]oseltamivir and [^{11}C]Ro 64-0802 has been previously published by us elsewhere [22]. Briefly, [^{11}C]AcCl [23], a labeling agent for radiosynthesis, was prepared by reacting methylmagnesium bromide with [^{11}C]CO_2, followed by chlorination with oxalyl chloride [24]. Purified [^{11}C]AcCl was reacted with the precursor [22] in the presence of Et_3N for 3 min at 80°C, followed by treatment with 6 N HCl. After the two-step reactions, the radioactive mixture was purified by HPLC [Waters XBridge Prep C18 5 μm column, 10 mm ID×250 mm, $CH_3CN/H_2O/Et_3N$ (30/70/1), 5 ml/min, 254 nm] to give [^{11}C]oseltamivir. [^{11}C]Oseltamivir was then hydrolyzed with 1% NaOH for 5 min at 100°C to yield [^{11}C]Ro 64-0802. From the end of bombardment, the synthesis times of [^{11}C]oseltamivir and [^{11}C]Ro 64-0802 were about 30 and 35 min, respectively. Starting from cyclotron-produced [^{11}C]CO_2 of 30–37 GBq, [^{11}C]oseltamivir (n=5) or [^{11}C] Ro 64-0802 (n=3) was produced with 450–1130 MBq as an injectable solution.

Radiochemical purity, identity and specific activity were assayed by analytical HPLC (CAPCELL PAK C_{18} column: 4.6 mm ID×250 mm). The retention time (t_R) was 6.5 min for [^{11}C]oseltamivir [$CH_3CN/H_2O/Et_3N$ (30/70/0.1), 1.0 ml/min, 254 nm] and 5.2 min for [^{11}C]Ro 64-0802 [CH_3OH/pH 6.8 phosphate buffer (4/6), 1.0 ml/min, 210 nm], respectively. The identity was confirmed by coinjecting with the corresponding nonradioactive sample. Radiochemical purity was >98% for [^{11}C]oseltamivir (n=5) and >97% for [^{11}C]Ro 64-0802 (n=3), and the specific activity was averaged to be 8.9 GBq/μmol as determined from the mass measured from HPLC UV analysis.

2.3. Animals

Male mice weighing 30–40 g (ddY, 7–8 weeks, SLC, Shizuoka, Japan) were used. The animals were maintained and handled in accordance with recommendations by the U. S. National Institutes of Health and our guidelines (National Institute of Radiological Sciences, NIRS, Chiba, Japan). The studies were approved by the Animal Ethics Committee of NIRS.

2.4. Biodistribution study

2.4.1. Dissection method

A saline solution of [^{11}C]oseltamivir or [^{11}C]Ro 64-0802 (average, 15 MBq/200 μl) was injected into mice through the tail vein. Four mice were sacrificed by cervical dislocation at 1, 5, 15, 30 or 60 min after injection. The whole-brain, liver, lung, heart, kidney, stomach, small intestine, spleen, large intestine, muscle and blood samples were quickly removed. The radioactivity present in these tissues was measured using a 1480 Wizard gamma counter (PerkinElmer Japan, Yokohama, Japan) and expressed as a percentage of the injected dose per gram of wet tissue (% ID/g; mean±S.D., n=4). All radioactivity measurements were corrected for decay.

2.4.2. Micro-PET

PET scans were performed using a small-animal PET Inveon scanner (Siemens Medical Solutions USA, Knoxville, TN). These experiments were performed three times for each ligand using different mice (n=3). Prior to the scans, the mice were anesthetized with 1.5% (v/v) isoflurane. After transmission scans for attenuation correction for 2 cycles (803 s) using a ^{57}Co point source, dynamic emission scans were acquired over 90 min in a 3D list mode with an energy window of 350–650 keV. [^{11}C]Oseltamivir or [^{11}C]Ro 64-0802 (average, 15 MBq/100–300 μl) was injected via the tail vein, while the animals were positioned on the scanner bed before a dynamic PET study was acquired for 90 min. All list-mode data were sorted into 3D sinograms, which were then Fourier rebinned into 2D sinograms (frames, 4×1, 8×2 and 20×5 min). Dynamic images were reconstructed with filtered back-projection using a Ramp filter. Regions of interest (ROIs) were placed on the brain, lung, heart, liver, kidney and so forth using ASIPro VM (Analysis Tools and System Setup/Diagnostics Tool; Siemens Medical Solutions USA).

Time–activity curves (corrected for decay) in the organs were obtained for each scan. For image analysis, CAPP software, version 7.1 (CTI/Siemens), was used. Images were calibrated to standardized uptake values (SUVs) or to units of becquerel per milliliter. The SUV was calculated according to the following formula: measured activity concentration (Bq/ml)×body weight (g)/injected activity (Bq).

2.5. Metabolite assay in plasma and brain homogenate

2.5.1. In vitro

After mice (n=3 for each ligand) were sacrificed by cervical dislocation, blood and whole-brain samples were removed quickly from mice. A blood sample was centrifuged at 15,000 rpm for 2 min at 4°C to separate plasma, 300 μl of which was collected and stored at 0°C until used. The brain was homogenized in threefold volume of 50 mM phosphate buffer (pH 7.4) and also stored at 0°C until used. The plasma and brain homogenate should be used for incubation within 30 min, respectively.

After preincubation of plasma (130 μl) and brain homogenate (200 μl) at 37°C for 5 min, [^{11}C]oseltamivir or [^{11}C]Ro 64-0802 (0.4 MBq/0.24 nmol/10 μl) was added to the tissues, respectively. At 1, 5, 15 and 30 min after incubation, 15 μl of the incubation mixture was withdrawn and immediately added to 45 μl of CH_3CN. The mixture was vortexed for deproteination within 15 s and centrifuged at 15,000 rpm for 2 min at 4°C. The supernatant was collected for analysis.

An aliquot of the supernatant (10 μl) prepared from the plasma or brain homogenate was developed in the following thin-layer chromatography (TLC) mobile phase: $CHCl_3$/CH_3OH/AcOH (5/2/0.1). The TLC plate was air-dried and placed in contact with a imaging plate (BAS-MS2025, FUJIFILM Co., Tokyo) for 60 min, and the radioactivity distribution on the plate was analyzed using a "Bio-Imaging Analyzer (BAS-5000, FUJIFILM Co.). The percentage of [^{11}C]oseltamivir (R_f: 0.75) or [^{11}C]Ro 64-0802 (R_f: 0.38) to total radioactivity on the TLC chromatogram was calculated as %=(peak area for [^{11}C]ligand/total peak area)×100.

After radioactivity decay, the protein concentration in each incubation mixture was measured by the Lowry method. From [^{11}C]oseltamivir experiment, the formation rate of [^{11}C]Ro 64-0802 in plasma protein and brain protein was calculated as:

$$F = (A \times R)/(100 \times P \times T)$$

where F is the [^{11}C]Ro 64-0802 formation rate (pmol/min/mg protein), A is the amount of [^{11}C]oseltamivir added to the incubation mixture (pmol), R is the percentage of [^{11}C]Ro 64-0802 at an observation time point (%), P is the protein concentration in plasma or brain incubation mixture (mg protein/tube) and T is the observation time (min).

2.5.2. In vivo

After intravenous injection of [^{11}C]oseltamivir (30–44 MBq/200–300 μl) into mice (n=3), these mice were sacrificed by cervical dislocation at 1, 5, 15 and 30 min. Blood (0.5–1.0 ml) and whole-brain samples were removed quickly. The blood sample was centrifuged at 15,000 rpm for 2 min at 4°C to separate plasma, which (300 μl) was collected in a test tube containing CH_3CN (300 μl). After the tube was vortexed for 15 s and centrifuged at 15,000 rpm for 2 min for deproteinization, the supernatant was collected and diluted with the same amount of distilled water for analysis. At the same time, the mouse brains were homogenized in twofold volume of ice-cooled phosphate buffer (pH 7.4) solution. The homogenate was centrifuged at 15,000 rpm for 2 min at 4°C, and the supernatant was collected and deproteinized for analysis.

An aliquot of the sample (100–500 μl) prepared from the plasma or brain homogenate was injected into the analytic HPLC system and analyzed for [^{11}C]oseltamivir under the same conditions described above except for a flow rate of 1.5 ml/min. The percentage of [^{11}C]oseltamivir (t_R=5.6 min) or [^{11}C]Ro 64-0802 (t_R=2.4 min) to total radioactivity (corrected for decay) on the HPLC chromatogram was

calculated as %=(peak area for [^{11}C]ligand/total peak area)×100. The recovery ratio of radioactivity eluted from the HPLC column was >95% for the plasma and brain homogenate samples.

3. Results

3.1. Biodistribution

The biodistribution of [^{11}C]oseltamivir and [^{11}C]Ro 64-0802 in mice was measured as the decay-corrected percentage injected activity per gram of tissue (% ID/g).

Fig. 2A shows the data of [^{11}C]oseltamivir in 11 specific regions of mice. After the tracer injection, high initial uptake of radioactivity was found in the blood, lung and heart, followed by a rapid decrease of radioactivity in these organs. Radioactivity accumulated in the liver, small intestine and kidney from the early time point, peaked at about 15 min and declined until the end of this experiment. The maximum level of radioactivity was detected in the kidney among all the organs examined. Compared to other peripheral organs, relatively low uptake was measured in the spleen, stomach and muscle. Radioactivity accumulated in the large intestine over time. The lowest radioactivity was found in the brain (0.20±0.01% at 1 min, 0.16±0.01% at 5 min, 0.14±0.01% at 15 min, 0.09±0.02% at 30 min and 0.06±0.02% ID/g at 60 min after injection). Despite the low level, the decrease rate of radioactivity in the brain was much slower than that in the blood. Calculated from the averaged weight (0.45 g) of the mouse brains used here, 0.09–0.027% of injected [^{11}C] oseltamivir was present in the whole brains between 1 and 60 min after injection.

Fig. 2B shows the data of [^{11}C]Ro 64-0802 in the same regions as in the [^{11}C]oseltamivir experiment. [^{11}C]Ro 64-0802 displayed higher initial radioactivity in the blood and then faster washout from the blood than [^{11}C]oseltamivir described above. A high level of radioactivity was detected in the kidney, which decreased rapidly from 5 min after the tracer injection. Except in the kidney, radioactivity concentration in the other organs was extremely low. In the brain, radioactivity was 0.39±0.08% at 1 min, 0.19±0.06% at 5 min, 0.08±0.01% at 15 min, 0.06±0.02% at 30 min and 0.03±0.01% ID/g at 60 min after injection. Calculated from the averaged weight (0.45 g) of the mouse brains used here,

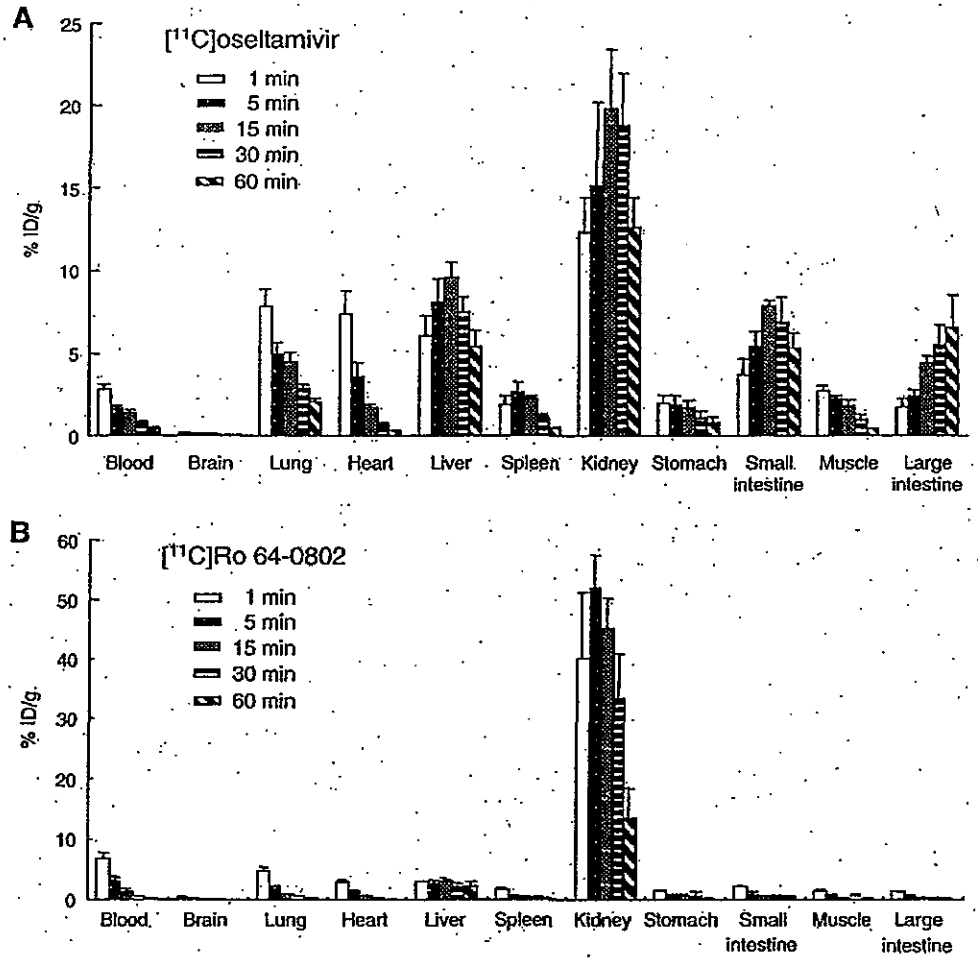

Fig. 2. Biodistribution in mice (n=4 for each ligand) by the dissection method. Radioactivity was expressed as the percentage of the injected dose per gram of tissue or organ (% ID/g; mean±S.D., n=4). (A) [^{11}C]oseltamivir. (B) [^{11}C]Ro 64-0802.

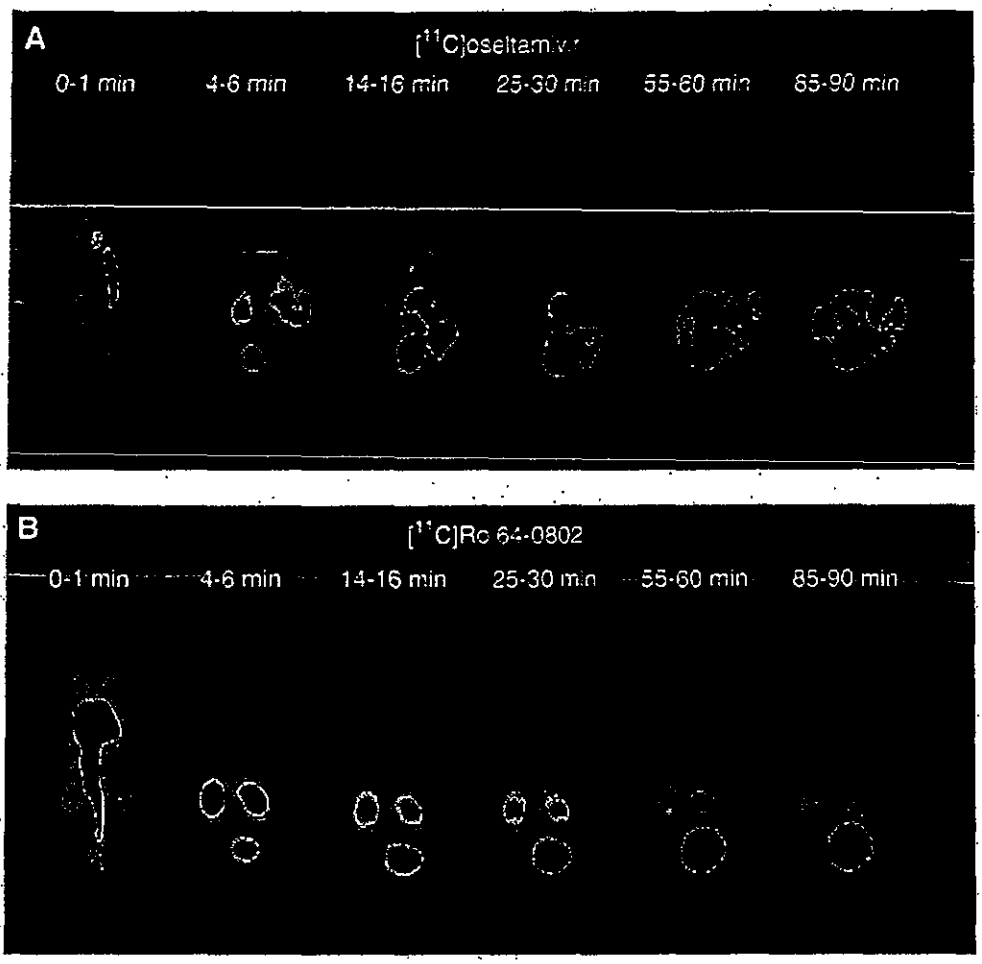

Fig. 3. Typical static micro-PET images at different time points after tracer injection. (A) [^{11}C]oseltamivir. (B) [^{11}C]Ro 64-0802. PET scans were performed for three mice for each ligand.

0.176–0.014% of injected [^{11}C]Ro 64-0802 was present in the whole brains within this experiment.

3.2. Micro-PET

The biodistribution of [^{11}C]oseltamivir and [^{11}C]Ro 64-0802 in mice was determined by micro-PET scans. All micro-PET images were corrected for decay. Fig. 3 shows two typical PET images of mice at different time points after injection of [^{11}C]oseltamivir (Fig. 3A) and [^{11}C]Ro 64-0802 (Fig. 3B). The injected dosing solution was carried through the vena cava to the heart, and then [^{11}C] oseltamivir or [^{11}C]Ro 64-0802 was distributed to the whole body. At 1 min after the [^{11}C]oseltamivir injection (Fig. 3A), radioactivity immediately appeared in the lung, heart and kidneys. Uptake in these organs peaked rapidly and was then eliminated. Radioactivity accumulation in urinary bladder represented rapid and significant excretion in urine. High radioactivity in the liver, gall bladder and small intestine from the early time period also suggested biliary excretion of radioactivity. Radioactive concentrations in liver and other tissues and organs, except digestive organs and urinary bladder, decreased gradually around 16 min after injection. On the other hand, after the injection of [^{11}C]Ro 64-0802, the renal elimination pathways dominated the whole-body distribution. Most radioactivity

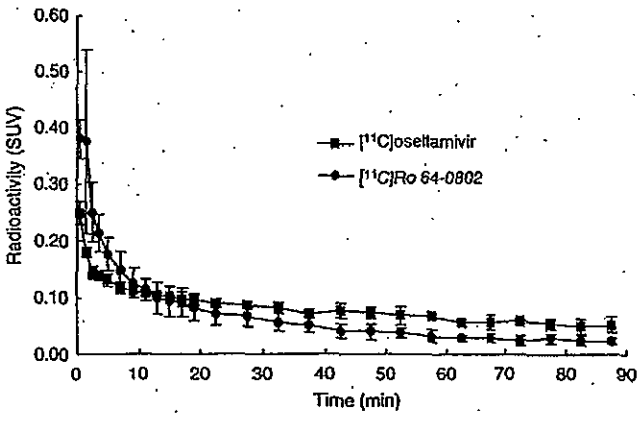

Fig. 4. Time–activity curves of [^{11}C]oseltamivir and [^{11}C]Ro 64-0802 in mouse brains (n=3 for each ligand). Radioactivity was detected and expressed as SUV. The SUV (mean±S.D., n=3) was calculated according to the following formula: measured activity concentration (Bq/ml)×body weight (g)/injected activity (Bq).

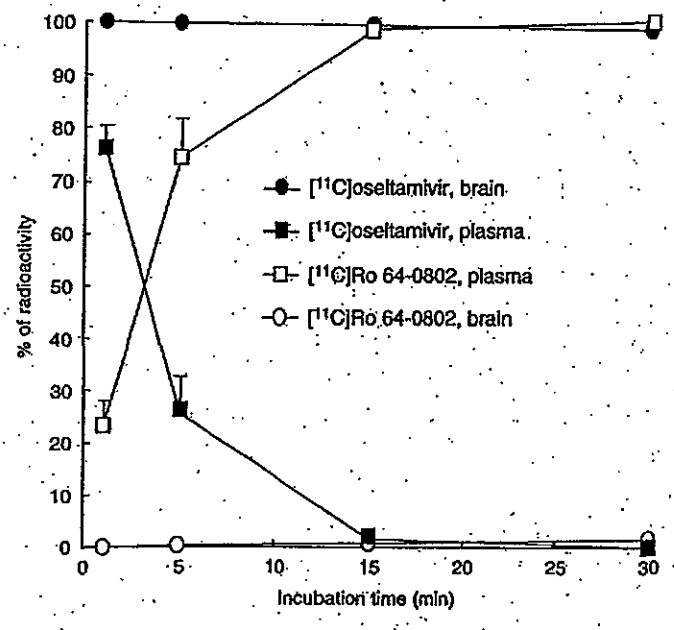

Fig. 5. Percentage (mean±S.D., n=3) of [^{11}C]oseltamivir and [^{11}C]Ro 64-0802 in the plasma and brain homogenate of mice (n=3) at four time points after incubation of [^{11}C]oseltamivir.

was rapidly cleared from the kidneys and directly excreted by the bladder.

Quantitative results of the radioactivity concentrations of [^{11}C]oseltamivir and [^{11}C]Ro 64-0802 in the brains over time are shown in Fig. 4. Despite the relatively high initial uptake, about 50% of highest radioactivity in the brain had rapidly decreased by 5 min after the injection of both ligands. After this phase of initial rapid decline, from 10 min to the end (90 min) of the PET experiments, the radioactivity level in the brains decreased slowly, from SUV 0.11 to 0.05 for [^{11}C] oseltamivir and from SUV 0.12 to 0.02 for [^{11}C]Ro 64-0802.

3.3. Metabolite assay

Fig. 5 shows the in vitro metabolic results of [^{11}C] oseltamivir and [^{11}C]Ro 64-0802 in the plasma and brain homogenate of mice. After incubation of [^{11}C]oseltamivir with plasma, [^{11}C]oseltamivir was rapidly metabolized to [^{11}C]Ro 64-0802. The fraction corresponding to unmetabolized [^{11}C]oseltamivir in the plasma decreased to 25% at 5 min and had almost disappeared at 15 min. In the brain homogenate, [^{11}C]oseltamivir displayed a slight decrease over time. [^{11}C]Ro 64-0802 was identified with radio-TLC as the main radioactive metabolite. Fig. 6 shows the amounts of [^{11}C]Ro 64-0802 produced by the enzymatic hydrolysis of [^{11}C]oseltamivir in the plasma (Fig. 6A) and brain homogenate (Fig. 6B). The formation rate of [^{11}C]Ro 64-0802 in the plasma by 5 min was calculated as 5.1 pmol/min/mg protein. In the brain homogenate, its formation rate by 15 min was calculated as 0.02 pmol/min/mg protein. The in vitro enzymatic activity hydrolyzing [^{11}C]oseltamivir to [^{11}C]Ro 64-0802 in the brain was about 250 times lower than that in the plasma.

On the other hand, [^{11}C]Ro 64-0802 was stable when exposing this ligand to the plasma and brain homogenate for 30 min.

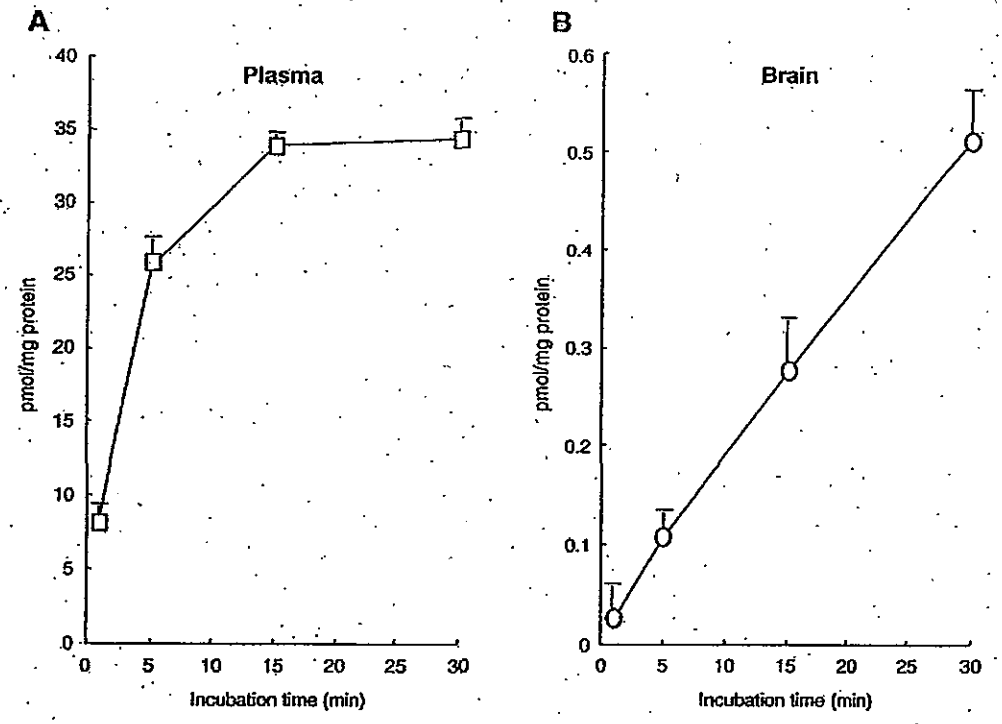

Fig. 6. Amounts (mean±S.D., n=3) of [^{11}C]Ro 64-0802 produced by enzymatic hydrolysis of [^{11}C]oseltamivir in the plasma (A) and brain homogenate (B) of mice (n=3) at four time points after incubation of [^{11}C]oseltamivir.